DOI: 10.1002/ejic.201100475

Hierarchical Durian-Shaped Dodecahedral Rutile Microparticles

Jia Liu,[a] Xianfeng Yang,[a,b] Yuping Wen,[a] Qiong Gao,[a] Qiang Zhou,[a] Chaolun Liang,[a] and Mingmei Wu*[a]

Keywords: Nanostructures / Hydrothermal synthesis / Titanium / Rutile / Hierarchical structures

Hierarchical durian-shaped dodecahedrons of rutile have been synthesized hydrothermally from titanium *n*-butoxide (TNB) in oxalic acid. The products are characterized by powder X-ray diffraction (PXRD), scanning electron microscopy (SEM), transmission electron microscopy (TEM) and selected-area electron diffraction (SAED) and the hierarchical architectures of these dodecahedrons have been addressed. It is suggested that the growth of the hierarchical rutile architectures is directly from a precursor, titanium oxide oxalate hydroxide hydrate [$Ti_2O_2(C_2O_4)(OH)_2{\cdot}H_2O$, briefly denoted as TOOHH], which can be formed at an earlier stage during hydrothermal synthesis, typically at lower reaction temperature. The production of the novel hierarchical nanostructure is attributed to epitaxial growth along some specific directions and the chemical etching and growth is due to similarities of corner-sharing TiO_2 octahedrons between rutile and TOOHH.

Introduction

Titanium dioxide (TiO_2) nanomaterials have been extensively used in photocatalysis,[1–5] photocells,[6] hydrogen storage[7,8] and chemical sensors[9–11] over past decades. The fabrication of TiO_2 nanomaterials has attracted more and more attention. Many different nanostructures of titanium dioxide such as nanoparticle,[12] nanorods,[13,14] nanotubes,[15–18] hollow nanospheres[19] and nanotrees[20] have been chemically prepared and the experimental results have indicated that their properties are generally related to crystal phases, sizes, shapes, growth orientations, assemblies and so on.[21–25] Therefore, the controlled growth of unique TiO_2 nanostructured materials is quite essential.

TiO_2 exists as three polymorphs in nature: anatase, brookite and rutile. The key difference in their crystallographic structures is the linkage of TiO_6 octahedrons, all of which are composed of a titanium(Ti) atom in the centre and six surrounding oxygen(O) atoms.[22] In anatase, each TiO_6 octahedron connects with eight others−four edge-sharing and four corner-sharing−whereas in brookite, each TiO_6 connects with nine others, three edge-sharing and six corner-sharing. In rutile, each TiO_6 connects with ten others, two edge-sharing and eight corner-sharing. There is more corner-sharing behaviour with each TiO_6 octahedron in rutile relative to the two other polymorphs.

Hydrothermal synthesis has been widely used in the growth of titania nanocrystals with a view toward crystal phases and novel architectures. By changing the hydrothermal growth conditions, various TiO_2 nanomaterials with specific morphologies could be prepared and crystal sizes could be readily tuned.[12,26,27] Rutile or anatase nanocrystals with different sizes could be hydrothermally grown from titanium tetrachloride by changing the concentrations of the reaction source (i.e., titanium tetrachloride) and other hydrothermal reaction conditions.[26] Rutile is the most thermodynamically stable phase, and anatase can be transferred into rutile. Zhu and his co-workers investigated the conversion of TiO_2(B) to anatase and rutile, respectively.[28] Rutile nanomaterials are generally prepared in the presence of a strong acid medium, typically with the assistance of either hydrochloric acid or nitric acid.[20,29,30] For example, rutile nanotree arrays are grown by means of hydrochloric acid vapour oxidation.[20] Complex flowerlike and leaflike rutile TiO_2 nanoarchitectures have been obtained by facile hydrothermal growth in hydrochloric acid.[29] Previously, rutile nanobamboo raft arrays were yielded by topotactic conversion from a layer-structured precursor in which there were segments analogous to those in rutile.[30] By varying the pH values of the reaction media, the selective growth of different TiO_2 phases was suggested to be on account of the growth units in different pH values serving as structural segments for either anatase, brookite or rutile.[31] It was proposed that anatase was directly

[a] MOE Key Laboratory of Bioinorganic and Synthetic Chemistry, State Key Laboratory of Optoelectronic Materials and Technologies, School of Chemistry and Chemical Engineering and Instrumental Analysis and Research Centre, Sun Yat-Sen (Zhongshan) University, Guangzhou 510275, P. R. China
Fax: +86-20-84111038
E-mail: ceswmm@mail.sysu.edu.cn
[b] Institute of Bioengineering and Nanotechnology, 31 Biopolis Way, The Nanos, 09-01, Singapore 138669
Supporting information for this article is available on the WWW under http://dx.doi.org/10.1002/ejic.201100475.

formed from TiO_2(B) in dilute acid medium due to the structural analogy, whereas rutile was yielded in concentrate acid after structural re-stacking of TiO_6 octahedrons to attain a structural similarity with segments in rutile. Although rutile nanomaterials were also prepared in oxalic acid solution, they were usually assisted by the strong acid and the morphology of nanomaterials was difficult to control.[32–34] In this contribution, hierarchically durian-shaped rutile micropolyhedrons have been grown through hydrothermal synthesis in oxalic acid solution, a weak acid. The production of the novel hierarchical polyhedral nanostructure is attributed to epitaxial growth from a precursor, titanium oxide oxalate hydroxide hydrate $[Ti_2O_2(C_2O_4)(OH)_2 \cdot H_2O$, briefly denoted as TOOHH].[30]

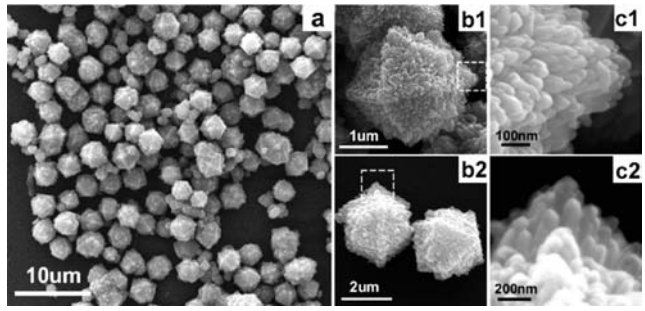

Figure 2. SEM images of the product with diffraction magnifications. (a) Low magnification for a large-area view. (b) A single microparticle and two individual ones with diffraction-view directions; they are dodecahedrally similar. (c) Enlargements of the white squares in (b1) and (b2), respectively.

Results and Discussion

The product isolated after hydrothermal crystallization at 220 °C for four days was characterized by powder X-ray diffraction (PXRD) at first. The PXRD pattern matches well with JCPDS card no. 21-1276 for tetragonal rutile TiO_2 with $a = b = 0.4593$ nm and $c = 0.2958$ nm (Figure 1). The SEM image shows that the product consists of a large amount of uniform durian-like dodecahedral microparticles dimensions of around 2.0 μm (Figure 2, a). From a close-up view of typical particles (Figure 2, b), it can be seen that each of them is not a real polyhedral single crystal but is composed of nanothorn arrays on each side surface, which resemble durian surfaces. The nanothorns at each ridge and vertex are highly aligned (Figure 2, c). The hierarchical nanostructure was further analyzed by cross-section TEM and electron microscopy (Figure 3).

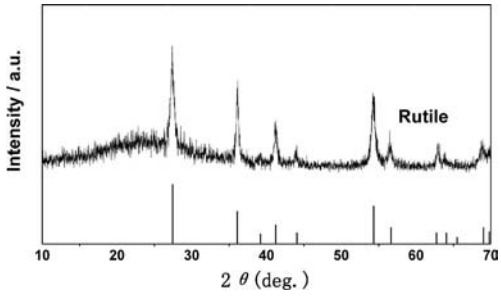

Figure 1. PXRD pattern of the product obtained through a typical hydrothermal growth at 220 °C for 4 d. The bars are from JCPDS card no. 21-1276 for rutile TiO_2.

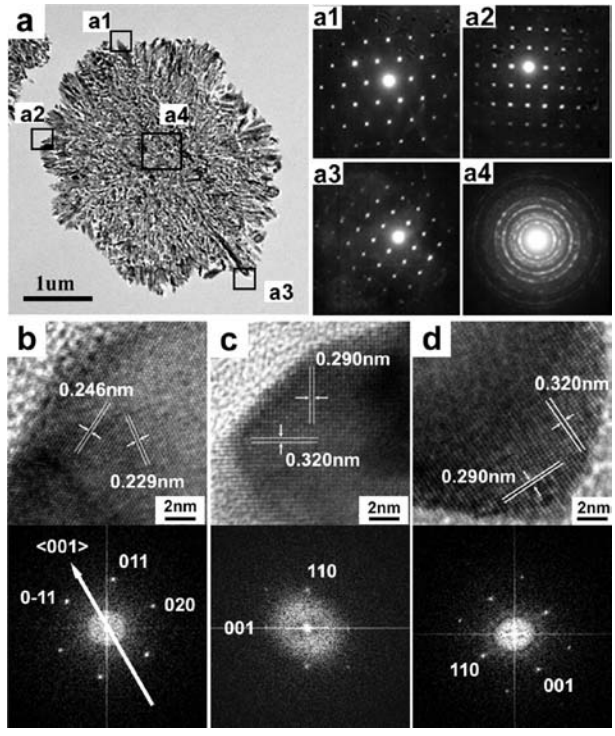

Figure 3. (a) TEM images of a cross-section of a single microparticle. (a1–a4) SAED patterns from corresponding areas in (a). (b–d) HRTEM images from corresponding areas (a1–a3), respectively. In the bottom row are the related fast-Fourier transform (FFT) patterns.

From Figure 3 (a), it is clear that each dodecahedral microparticle is constructed of radial arrays of nanothorns. A close-up view of the edges of the particle indicates that these nanothorns are aligned on some specific orientation and there are some specific relationships between nanothorn arrays. The selected-area electron diffraction (SAED) patterns (Figure 3, a1–a4) and the high-resolution TEM images (Figure 3, b–d) from the black solid-lined squares in Figure 3a suggest these nanorods are single crystals with tiny tips. The distinguishable lattice spacings of 0.246, 0.229, 0.290 and 0.320 nm in the HRTEM images correspond to the {101}, {200}, {001} and {110} lattice planes of rutile, respectively. Combined with the related FFT patterns at the bottom of Figure 3, each nanothorn is confirmed to have grown along its {001} direction. The SAED pattern (Figure 3, a4) from the centre of the nanoparticle (Figure 3, a) is neither a single-crystal feature nor a common polycrystal feature due to some strong diffraction spots on diffraction rings. This pattern implies that the microparticle is built up by radically orientated nanorods. The hierarchical nanostructure is quite complex but it is possible to be simulated.

To investigate the growth mechanism of the above rutile product, the temperature and time of the hydrothermal reaction were changed (Figure 4). If our hydrothermal reaction was carried out at 140 °C only for one day, a product that was suggested to be orthorhombic TOOHH (JCPDS card no. 48-1164; a = 1.0503 nm, b = 1.5509 nm and c = 0.97 nm; $\alpha = \beta = \gamma = 90°$) was yielded (Figure 4, a). The thermal analysis of the precursor is given in Figure S1 in the Supporting Information. From the SEM image (Figure 5, a), it can be observed that the crystals appear in hexagonal microprisms with a diameter of around 5 μm. With further autoclaving treatment for 4.0 d, a white product was yielded that was characterized to be rutile TiO_2 (see parts b in Figures 4 and 5). The product also crystallized in polyhedral particles with unsmooth surfaces. The particle microstructures are quite similar to those in Figure 2 but they do not appear as uniform and elegant as those in Figure 2. The growth conditions shown in Figures 1 and 2 may be the optimal ones for the yield of the above-mentioned durian-like dodecahedral microparticles. The SEM pictures of the products grown after crystallization for two and three days are presented in Figure S2 in the Supporting Information.

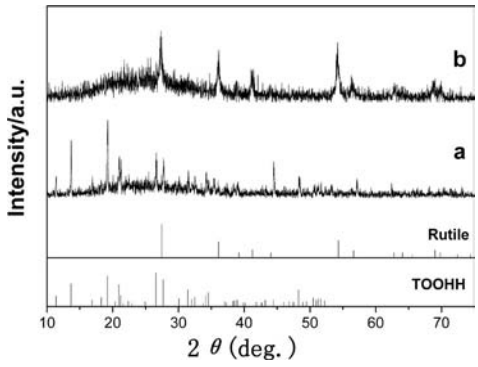

Figure 4. (a,b) PXRD patterns of the product obtained after hydrothermal treatment for 1 d and 4 d, respectively. The bars are from JCPDS card no. 48-1164 for TOOHH and JCPDS card no. 21-1276 for rutile.

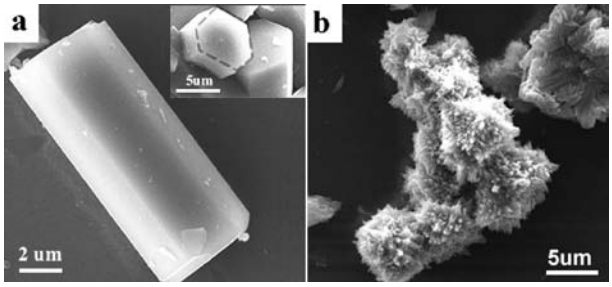

Figure 5. (a) SEM images of TOOHH particles with side surface and cross-section obtained by hydrothermal reaction at 140 °C for 1 d. (b) SEM image of rutile particles obtained by hydrothermal reaction at 140 °C for 4 d.

Upon inspecting the crystal structure of the precursor, TOOHH (c-centred orthorhombic), it is found that all the TiO_6 octahedrons connect to adjacent ones by corner-sharing. Interestingly, if the (100) lattice plane of TOOHH is viewed along the <100> direction, the arrangement of corner-sharing TiO_6 octahedrons is analogous to that of rutile. As shown in Figure 6, each channel along the <001> direction is a four-membered ring in rutile (Figure 6, b), whereas each channel along the <100> direction is a six-membered one in TOOHH (Figure 6, a). One six-membered ring can be assumed by the combination of two four-membered ones. Other structural resemblances are described in Figure 7. The corner–corner-linked octahedrons constitute zigzag chains along either the {010} or {001} directions with a screw-axis structure (Figure 7, a1, a2 and a1*, a2*), quite similar to that in rutile along the {001} direction (Figure 7, b). In addition, there are also zigzaglike chains connected by corner-sharing TiO_6 octahedrons along the {012} directions (Figure 7, a3 and a3*) that have a similar structure to that in rutile along the {001} direction through corner-sharing. It has been well established that rutile nanocrystals with 4_2 screw-axis crystallography along the c axis (Figure 7, b) are generally grown along the <001> direction.[12,27] This analogous connection behaviour to TiO_6 octahedrons can epitaxially promote the nucleation and growth of rutile along these eight original directions of TOOHH (i.e., two {001}, two {010} and four {012}, respectively). In TOOHH, there are corner-sharing TiO_6 dimmers along the {110} directions that are separated with each other by oxalate anions (Figure 7, c). Such structural segments have also a crystallographic relationship with those along the screw axis of rutile. Thus, epitaxial nucleation and growth of rutile nanocrystals may take place readily along the {110} directions with the extraction of oxalate anions.

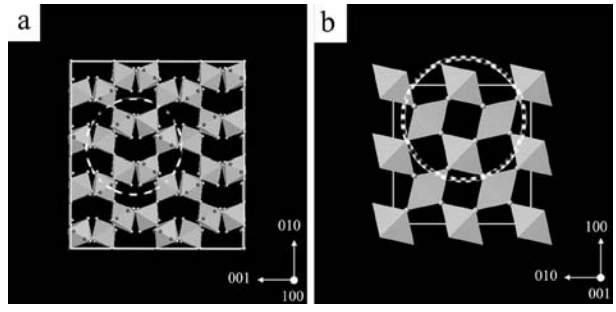

Figure 6. Comparison of crystallographic structures of (a) TOOHH and (b) rutile viewed along the a and c axes, respectively.

On the basis of the fundamental structural analyses above, the hierarchically dodecahedral rutile particles could be schematically illustrated as in Figure 8. Firstly, the two {001}, two {010} and four {012} directions of the precursor are in the same plane as shown in Figure 8 (a1). The angle between {001} and {012} is 17.2°. Secondly, there are four {110} directions shown in Figure 8 (a2), which has an acute angle of 45° with the plane. Inspection the schematic dodecahedron with the framework constructed by these directions as mentioned above (Figure 8, b–d) matches the profiles of the actual dodecahedrons quite well when viewed along a variety of directions (Figure 8, e–g). Therefore, it

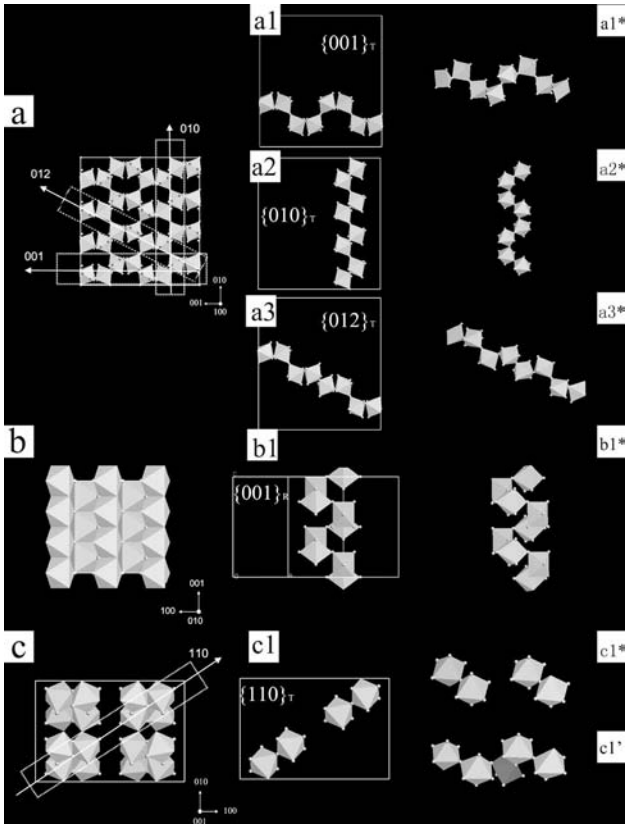

Figure 7. Comparison of the crystallographic structure of corner–corner-linked behaviours between (a,c) TOOHH and (b) rutile. (a) Connection of TiO_6 polyhedrons viewed along the *a* axis. (a1–a3) are some corner–corner-linked octahedron chains along the <001>, <010> and <012> directions of the (100) plane; (a1*–a3*) are views with slightly rotated directions for comparison. (b) Connection of TiO_6 polyhedrons in rutile viewed along the (010) direction; (b1) is a segmental chain with screw axis; (b1*) is depicted with a slight rotation for comparison. The picture in (c) is a unit cell of TOOHH along the <001> direction; (c1) is the side view of corner-sharing TiO_6 dimers; (c1*) is viewed from a different direction; and (c1′) is the intact chain as shown in (b1*) for epitaxial nucleation of rutile.

can be proposed that a durian-shaped dodecahedron is built by rutile nanothorn arrays, which can be considered to be grown epitaxially from TOOHH along its {001}, {010}, {012} and {110} planes during growth and aging.[30]

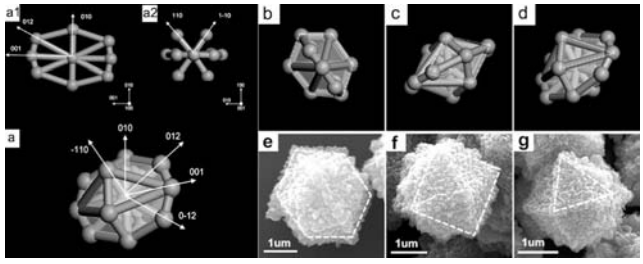

Figure 8. (a) Models for rutile dodecahedron growth. (b–d) Structural model of vivid microparticles viewed from different directions, accompanied by (e,f) corresponding SEM images.

Conclusion

Hierarchical durian-shaped dodecahedral microparticles of rutile TiO_2 have been synthesized by a hydrothermal reaction of titanium *n*-butoxide (TNB) in oxalic acid. It is suggested that the hierarchical rutile microparticles are grown epitaxially from a precursor [i.e., titanium oxide oxalate hydroxide hydrate (TOOHH)]. The epitaxial growth is assigned to the inherent structural resemblance of corner-shared TiO_6 octahedrons in TOOHH and rutile. The chains of corner-shared TiO_6 octahedrons in TOOHH along {001}, {010} and {012} show a similar arrangement to corner-shared TiO_6 along the <001> screw axis in rutile. In addition, the dimers of TiO_6 octahedrons connected by corner-sharing along the {110} direction also have a similarity to those in rutile along the <001> direction. Therefore, it can be considered that the durian-shaped dodecahedra built up by rutile nanothorn arrays are grown epitaxially along the {001}, {010}, {012} and {110} directions of TOOHH. This complex durian-shaped rutile nanostructure may show some distinguished functions such as photocatalysis on some specific organic molecules.[2]

Experimental Section

Chemical Synthesis: Titanium *n*-butoxide ($Ti(OC_4H_9)_4$, TNB) was used as the titanium source. It was chemically pure and all other chemicals were analytically pure. All of them were used without further purification. Quantitative oxalic acid (2.52 g) was dissolved in hot water (10 mL) and TNB (0.43 mL) was added into the oxalic acid solution drop-by-drop. A clear sol was obtained. Then the mixture was loaded into a Teflon-lined autoclave (20 mL) for hydrothermal growth. The resulting products were separated by centrifugation, washed with distilled water and dried at room temperature.

Structural Characterization: The structure of the as-obtained samples was characterized with XRD patterns, which were recorded with a Rigaku Dmax diffraction system with the use of Cu-K_α (λ = 1.54187 Å). Scanning electron microscopy (SEM) images were taken with an FEI Quanta 400 field-emission scanning electron microscope (FESEM, 15 kV) after the sample surface was coated by a novel metal such as gold. Transmission electron microscopy images were taken with a JEOL JEM-2010 transmission electron microscope (TEM) operated at 200 kV.

Supporting Information (see footnote on the first page of this article): TG-DTG curves of the precursor and SEM images of the products obtained after hydrothermal crystallization for 2 and 3 d, respectively.

Acknowledgments

This work was supported financially by the National Natural Science Foundation (NSFC) of China, the Government of Guangdong Province and Guangzhou City (grant numbers U0734002, 50872158, 8251027501000010 and 2010GN-CO11) and the Specialized Research Fund for the Doctoral Program of Higher Education (20090171110025).

[1] M. Kitano, M. Matsuoka, M. Ueshima, M. Anpo, *Appl. Catal. A* **2007**, *325*, 1–14.

[2] S. Yurdakal, G. Palmisano, V. Loddo, V. Augugliaro, L. Palmisano, *J. Am. Chem. Soc.* **2008**, *130*, 1568–1569.
[3] J. Jitputti, S. Pavasupree, Y. Suzuki, S. Yoshikawa, *J. Solid State Chem.* **2007**, *180*, 1743–1749.
[4] R. van de Krol, Y. Q. Liang, J. Schoonman, *J. Mater. Chem.* **2008**, *18*, 2311–2320.
[5] R. M. N. Yerga, M. C. A. Galvan, F. del Valle, J. A. V. de la Mano, J. L. G. Fierro, *ChemSusChem* **2009**, *2*, 471–485.
[6] W. R. Duncan, C. F. Craig, O. V. Prezhdo, *J. Am. Chem. Soc.* **2007**, *129*, 8528–8543.
[7] S. H. Lim, J. Z. Luo, Z. Y. Zhong, W. Ji, J. Y. Lin, *Inorg. Chem.* **2005**, *44*, 4124–4126.
[8] X. Hu, B. O. Skadtchenko, M. Trudeau, D. M. Antonelli, *J. Am. Chem. Soc.* **2006**, *128*, 11740–11741.
[9] E. Palomares, R. Vilar, A. Green, J. R. Durrant, *Adv. Funct. Mater.* **2004**, *14*, 111–115.
[10] I. A. Al-Homoudi, J. S. Thakur, R. Naik, G. W. Auner, G. Newaz, *Appl. Surf. Sci.* **2007**, *253*, 8607–8614.
[11] M. R. Mohammadi, D. J. Fray, M. C. Cordero-Cabrera, *Sens. Actuators,. B* **2007**, *124*, 74–83.
[12] M. M. Wu, G. Lin, D. H. Chen, G. G. Wang, D. He, S. H. Feng, R. R. Xu, *Chem. Mater.* **2002**, *14*, 1974–1980.
[13] M. H. Imanieh, Y. Vahidshad, P. Nourpour, S. Shakesi, K. Shabani, *NANO* **2010**, *5*, 279–285.
[14] A. S. Attar, M. S. Ghamsari, F. Hajiesmaeilbaigi, S. Mirdamadi, K. Katagiri, K. Koumoto, *Mater. Chem. Phys.* **2009**, *113*, 856–860.
[15] X. J. Xu, X. S. Fang, T. Y. Zhai, H. B. Zeng, B. D. Liu, X. Y. Hu, Y. Bando, D. Golberg, *Small* **2011**, *7*, 445–449.
[16] H. Wen, Z. F. Liu, Q. B. Yang, Y. X. Li, J. Yu, *Electrochim. Acta* **2011**, *56*, 2914–2918.
[17] E. Feschet-Chassot, V. Raspal, Y. Sibaud, O. K. Awitor, F. Bonnemoy, J. L. Bonnet, J. Bohatier, *Thin Solid Films* **2011**, *519*, 2564–2568.
[18] S. P. Albu, H. Tsuchiya, S. Fujimoto, P. Schmuki, *Eur. J. Inorg. Chem.* **2010**, 4351–4356.
[19] H. X. Li, Z. F. Bian, J. Zhu, D. Q. Zhang, G. S. Li, Y. N. Huo, H. Li, Y. F. Lu, *J. Am. Chem. Soc.* **2007**, *129*, 8406–8407.
[20] X. F. Yang, J. L. Zhuang, X. Y. Li, D. H. Chen, G. F. Ouyang, Z. Q. Mao, Y. X. Han, Z. H. He, C. L. Liang, M. M. Wu, J. C. Yu, *ACS Nano* **2009**, *3*, 1212–1218.
[21] Z. B. Zhang, C. C. Wang, R. Zakaria, J. Y. Ying, *J. Phys. Chem. B* **1998**, *102*, 10871–10878.
[22] X. Chen, S. S. Mao, *Chem. Rev.* **2007**, *107*, 2891–2959.
[23] N. Murakami, Y. Kurihara, T. Tsubota, T. Ohno, *J. Phys. Chem. C* **2009**, *113*, 3062–3069.
[24] C. T. Dinh, T. D. Nguyen, F. Kleitz, T. O. Do, *ACS Nano* **2009**, *3*, 3737–3743.
[25] H. G. Yang, H. C. Zeng, *J. Phys. Chem. B* **2004**, *108*, 3492–3495.
[26] Y. Q. Zheng, E. R. Shi, Z. Z. Chen, W. J. Li, X. F. Hu, *J. Mater. Chem.* **2001**, *11*, 1547–1551.
[27] X. F. Yang, H. Konishi, H. F. Xu, M. M. Wu, *Eur. J. Inorg. Chem.* **2006**, *11*, 2229–2235.
[28] H. Y. Zhu, Y. Lan, X. P. Gao, S. P. Ringer, Z. F. Zheng, D. Y. Song, J. C. Zhao, *J. Am. Chem. Soc.* **2005**, *127*, 6730–6736.
[29] H. B. Li, X. C. Duan, G. C. Liu, X. B. Jia, X. Q. Liu, *Mater. Lett.* **2008**, *62*, 4035–4037.
[30] X. F. Yang, C. Karthik, X. Y. Li, J. X. Fu, X. H. Fu, C. L. Liang, N. Ravishankar, M. M. Wu, G. Ramanath, *Chem. Mater.* **2009**, *21*, 3197–3201.
[31] K. Tomita, V. Petrykin, M. Kobayashi, M. Shiro, M. Yoshimura, M. Kakihana, *Angew. Chem. Int. Ed.* **2006**, *45*, 2378–2381.
[32] Y. V. Kolen'ko, V. D. Maximov, A. V. Garshev, P. E. Meskin, N. N. Oleynikov, B. R. Churagulov, *Chem. Phys. Lett.* **2004**, *388*, 411–415.
[33] C. Malitesta, A. Tepore, L. Valli, A. Genga, T. Siciliano, *Thin Solid Films* **2002**, *422*, 112–119.
[34] Y. V. Kolen'ko, A. A. Burukhin, B. R. Churagulov, N. N. Oleinikov, *Inorg. Mater.* **2004**, *40*, 942–949.

Received: May 6, 2011
Published Online: August 31, 2011

